Ultrafine Selective Metal-Complexing Nanoparticles: Synthesis by Microemulsion Copolymerization, Binding Capacity, and Ligand Accessibility

Sonia Amigoni-Gerbier,[†] Sylvain Desert,[‡] Thadée Gulik-Kryswicki,[§] and Chantal Larpent*,[†]

SIRCOB ESA CNRS 8086, LRC CEA DSM 95-1, Université de Versailles St Quentin en Y., 45 Avenue des Etats-Unis, 78035 Versailles Cedex, France; Service de Chimie Moléculaire, CEA-Saclay, 91191 Gif sur Yvette Cedex, France; and Centre de Génétique Moléculaire, CNRS, 91198 Gif sur Yvette Cedex, France

Received July 30, 2001; Revised Manuscript Received November 28, 2001

ABSTRACT: Stable translucent aqueous suspensions of ligand-functionalized nanoparticles, with average diameters ranging from 12 to 20 nm and containing from 0.25 to up to 0.75 mmol of ligand/g, are readily obtained by copolymerization in oil-in-water microemulsions of a polymerizable tetraaza macrocycle, vinylbenzylcyclam (cyclam: 1,4,8,11-tetraazacyclotetradecane). These nanoparticles exhibit a very high selectivity for cupric ions with binding capacities of up to 0.65 mmol of Cu/g as well as a remarkable ligand accessibility, deduced from spectrophotometric titration, with about 75% of the cyclam residues located near the surface for nanoparticles in the 12−13 nm range. Core−shell bimetallic nanoparticles are obtained by cation exchange. The cyclam-functionalized nanoparticles are comparable to high-generation PAMAM dendrimers in their ability to complex metals.

Introduction

Polymer supports have been used in organic chemistry and catalysis for many years.[1−3] This technique has revolutionized organic synthesis in the past decade and created a new field known as combinatorial chemistry.[4,5] Since the activity of supported ligands, catalysts, or reagents depends on the accessibility of the active sites and is often limited by diffusion, considerable efforts have been made to develop new polymer supports with improved capacity, accessibility, and selectivity as well as suitable solvent affinity.[5−8] The past decade has witnessed a significant transformation in the area of particle science and technology with the emergence of nanoparticulate materials. The ability to control the surface characteristics of such nanoparticulate systems assumes paramount importance because of the high surface-to-volume ratio of the particles.[7]

In this context, the use of microemulsions as reaction media for the synthesis of polymers offers new opportunities. Indeed, the polymerization of oil component in oil-in-water microemulsions leads to polymer nanoparticles with diameters smaller than 30 nm and specific areas larger than 300 m^2/g.[9−11] Moreover, because of the well-defined structure of microemulsions, polymerization inside these systems allows one to control the structural properties of the resulting polymer and to synthesize special polymer materials, such as copolymers with high degrees of chemical functionalization, which are not accessible by other techniques.[9−18]

On the other hand, resin beads or latex-supported ligands as well as soluble ligand-functionalized macromolecules and dendrimers have been used as metal ion complexing agents[2,19−31] and proposed for an extensive variety of purposes as diverse as separation and recovery of metal ions,[2,20−24,27] catalysis,[2,25,26,28,29] dioxygen transport,[30] or sensors.[31] In this field the use of microemulsions as polymerization media offers new prospect for the development of efficient colloidal supports with improved specific area and ligand accessibilty. Two pioneer studies have shown that metal complexing nanoparticles in the 15−35 nm diameter range can be readily synthesized by a one-step copolymerization process with monomers containing a macrocycle[14] or a bipyridine unit.[16]

In this paper, we show that microemulsion copolymerization is a very useful method to produce stable aqueous suspensions of ultrafine selective metal-complexing nanoparticles with controlled size and adjustable metal-binding capacity. Using tetraazacyclotetradecane, so-called cyclam, as a ligand and its Cu(II) complex as a sensor, the complexation process can be monitored spectrophotometrically in the translucent aqueous suspensions of nanoparticles. The well-known cyclam ligand exhibits high affinities for transition metal cations[32] with thermodynamic stability constants in the order Cu(II) ≫ Ni(II) > other cations, an order that remains unchanged after anchoring to a polymer backbone or a resin.[22,23] We take advantage of the binding of cupric ions, which gives a very stable deep violet copper complex ($K = 10^{27}$), to study the capacity, accessibility, and selectivity of cyclam-functionalized nanoparticles.

Experimental Section

Synthesis of Vinylbenzylcyclam (1).[24] A mixture of cyclam (2 g, 10 mmol) and 100 mL of pure DMF was stirred at 100 °C for 20 min until complete dissolution. Vinylbenzyl chloride (70/30 mixture of meta and para isomers purchased from Fluka) (0.3 g, 2 mmol) in 4 mL of pure DMF was then added dropwise, and the mixture was stirred at 100 °C for 2 h. After cooling at room temperature, unreacted cyclam that precipitated was removed by filtration and the filtrate con-

[†] Université de Versailles St Quentin en Y.
[‡] CEA-Saclay.
[§] Centre de Génétique Moléculaire, CNRS.
* To whom correspondence should be addressed. Tel (33)-139254413; Fax (33)139254452; e-mail Larpent@chimie.uvsq.fr.

10.1021/ma0113632 CCC: $22.00
Published on Web 01/31/2002

centrated under vacuum (0.2 mmHg). The crude product was dissolved in light petroleum (50 mL) and washed with water (3 × 50 mL). The organic layer was separated, dried over $MgSO_4$, and concentrated under vacuum leading to **1** (0.5 g, 80%) as a white sticky liquid. TLC, $R_f = 0.8$ ($CHCl_3$/MeOH/NH_3, 2/2/1). GC/MS-EI (capillary column OV1, 260 °C; HP engine, 70 eV): tr = 29.1 and 30.8 min; (*m*/*z*): 99.2 (21), 117.1 (94), 160.2 (100), 317.2 (1). ^{1}H NMR ($CDCl_3$, 300 MHz) δ (ppm): 1.67 (m, 2H); 1.8 (m, 2H); 2.73 (broad, 20H); 5.25 (dd, $^3J = 11$ Hz, $^2J = 1$ Hz, 1H); 5.78 (dd, $^3J = 17.6$ Hz, $^2J = 1$ Hz, 1H); 6.70 (dd, $^3J = 17.6$ Hz, $^2J = 11$ Hz, 1H); 7.30 (m, 4H).

Preparation of the Cyclam-Functionalized Nanoparticles: Microemulsion Copolymerization. Styrene (**2**) and divinylbenzene (**3**) were purified by flash chromatography on silica gel (eluent cyclohexane) before use. The surfactant dodecyltrimethylammoniuim bromide, DTAB (purum, >98%), was purchased from Fluka and used without further purification.

Preparation of the Microemulsions. The microemulsions were prepared by adding under gentle magnetic stirring the mixture of monomers (0.4−0.83 g) to 20 g of a 15 wt % aqueous solution of DTAB. In every case a clear transparent microemulsion was obtained. When DMPA was used as the radical initiator, it was introduced in solution in the monomers blend before the preparation of the microemulsion. In sample C, 1.2 mL of NaOH (0.1 N) was added to the microemulsion before polymerization. The compositions of the starting microemulsions (wt %) are as follows: A, C, and F: water 81.7%, DTAB 14,4%, **1** 1%, **2** 1.3%, **3** 1.6%; B: water 81.9%, DTAB 14,4%, **1** 0.5%, **2** 1.6%, **3** 2%; D: water 81.6%, DTAB 14,4%, **1** 1%, **2** 3%; E: water 82.5%, DTAB 14,6%, **1** 1%, **2** 1.9%.

Polymerization. *Oil-Soluble Radical Initiator, 2,2-Dimethoxy-2-phenylacetophenone (DMPA)* (0.05 mol/mol of monomers, previously solubilized in the mixture of monomers): the freshly prepared microemulsion was transferred in a double-jacketed refrigerated 100 mL schlenck tube and degassed with nitrogen for 20 min. The polymerization was performed at 20 °C under white light irradiation using two 60 W lamps for 15 h.

Water-Soluble Radical Initiator, Ammonium Persulfate/Tetramethyldiaminomethane:[12,13] the freshly prepared microemulsion was transferred in a three-necked flask and degassed with nitrogen for 20 min. A solution of ammonium persulfate (0.06 mol/mol of monomers) in the minimum amount of water and pure tetramethyldiaminomethane (0.12 mol/mol of monomers) were then successively added. The polymerization was carried out at 20 °C for 15 h.

Gas chromatography[12,13] and thin-layer chromatography (light petroleum) indicated complete polymerization of all monomers. In every case, translucent stable suspensions are obtained.

Separation and Chemical Composition of the Resulting Polymers. 20 mL of methanol was added to 10 mL of suspension; the flocculated polymer was then separated by centrifugation (4000 rpm, 15 min). The resulting white paste was dispersed in demineralized water (100 mL) and heated at 60 °C overnight. After centrifugation, the crude polymer was washed twice again with water (2 × 100 mL) and dried at 50 °C until constant weight. The absence of remaining water was checked by ATG experiment (from 20 to 350 °C). The complete removal of the surfactant was checked by ^{1}H NMR and confirmed by the absence of bromine in elemental analysis. Elemental analyses have been obtained from the "Service Central d'Analyse" (CNRS, Vernaison, France). A: % C 82.80, % H 7.84, % N 3.52; C: % C 81.64, % H 8.48, % N 4.16; D: % C 85.16, % H 8.05, % N 4.01; E: % C 70.25, % H 6.61, % N 3.43. F: % C 84.67, % H 8.07, % N 2.97.

Competition Experiments were performed on suspension C according to the previously described procedure.[14] Briefly, about 10^{-2} mol of $Ni(NO_3)_2$, $Zn(NO_3)_2$, or $CoCl_2$ and 10^{-5} mol of $Cu(NO_3)_2$ were added to 5 g of suspension C, and the mixture was allowed to equilibrate. The resulting suspensions were then purified by dialysis (cellulose membranes, MWCO 3500). The metal-containing polymers were obtained after concentration to dryness and extensive washings with water followed by final drying with a purification yield of about 90%. The compositions of the isolated polymers are as follows: competition Ni/Cu: % C 75.22, % H 7.41, % N 3.99, % Ni 2.30, % Cu 0.51; competition Zn/Cu: % C 76.42, % H 7.54, % N 4.43, % Zn 2.39, % Cu 0.33; competition Co/Cu: % C 76.92, % H 7.42, % N 3.43, % Co 2.33, % Cu 0.30.

Metal Binding Capacity−Spectrophotometric Measurements. UV/vis analyses were performed on a Perkin-Elmer spectrophotometer UV/vis/NIR Lambda 19 equipped with a reflection sphere. Measurements were performed directly on the translucent suspensions resulting from polymerization. The spectra were recorded from 350 to 800 nm. In every case, the maximum absorption wavelength of the copper complex was observed at 536 ± 2 nm.

The ligand accessibility was studied by adding small aliquots (100−300 μL) of a 0.01 mol/L aqueous solution of copper nitrate to 2 g of suspension placed in a 1 cm quartz cell. The absorbance was measured 3 min after each addition. For the study of diffusion-limited complexation processes, similar titrations have been performed with 0.1 and 0.5 mol/L solutions of copper nitrate.

The metal binding capacity was deduced from the absorbance of the Cu complex at the equilibrium in the presence of stoichiometric amounts of copper nitrate (1 equiv of Cu per cyclam residue in the polymer as deduced from elemental analysis, copper concentration in the suspension $\sim (2-3) \times 10^{-2}$ mol/L). The same absorbance values were obtained when the complexation were performed in the presence of an excess of copper (10 equiv/cyclam) followed by removal of the unreacted cupric ions by dialysis (cellulose membrane, MWCO 3500) toward aqueous solutions of DTAB (15 wt %).

The spectroscopic study of the replacement of Zn(II) by Cu(II) was performed on a colorless suspension of Zn-containing 20 nm nanoparticles prepared by reacting an excess of $Zn(NO_3)_2$ with suspension C followed by removal of the unreacted Zn(II) salt by extensive dialysis toward an aqueous solution of DTAB (15%). The absorbance of the Cu−cyclam complex was measured until the equilibrium was reached.

Quasi-Elastic Light Scattering. The analyses were performed with a Brookhaven (BI2030AT correlator) equipped with an 2016 Ar laser (514.5 nm); the data were analyzed by the exponential sampling method or by the nonnegatively constrained least-squares multiple pass method (BI30atn software). The samples were diluted in pure water (0.2 mL of suspension in 100 mL of water) before analysis.

Freeze-Fracture Transmission Electron Microscopy. A 20−30 μm thick layer of the sample was deposited on a thin copper holder and then rapidly quenched in liquid propane. The frozen samples were fractured in vacuo (about 10^{-7} Torr) at liquid nitrogen temperature with the liquid nitrogen cooled knife inside a Balzers 301 freeze-etching unit. The replication was done using unidirectional shadowing with platinum−carbon at the angle of 35°. The mean thickness of the metal deposit was 1−1.5 nm. The replicas were washed with organic solvents and distilled water and then observed in a Philips EM 410 electron microscope. The contrast in images is related to the depth fluctuations of the metal deposit. The electron microscopy analyses have been performed on previously dialyzed suspensions: cyclam-functionalized nanoparticles were dialyzed toward DTAB (0.15 wt %), and metal-containing nanoparticles were dialyzed toward pure water.

Results and Discussion

I. Preparation and Characterization of Cyclam-Functionalized Nanoparticles. a. Preparation by Copolymerization in Microemulsion. Cyclam-functionalized nanoparticles are obtained by copolymerization of the polymerizable tetraaza macrocyclic derivative **1**, vinylbenzylcyclam, in oil in water microemulsions (Scheme 1). Microemulsions of mixture of monomer **1** and styrene **2**, with or without a cross-linking agent **3**, are prepared using a cationic surfactant DTAB (dodecyltrimethylammonium bromide)[14] and polymerized at room temperature using either an oil-soluble radical

Scheme 1. Synthesis of the Cyclam-Functionalized Nanoparticles and Copper Binding: (i) Copolymerization in Oil-in-Water Microemulsion, 3−4 wt %; (ii) Addition of Cupric Ion (or Other Metallic Cation) to the Aqueous Suspension

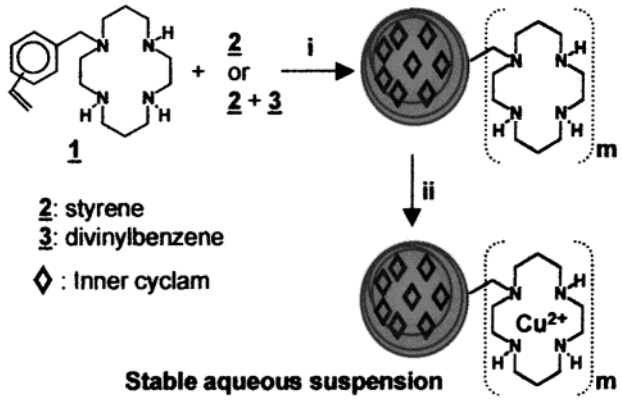

Table 1. Cyclam-Functionalized Nanoparticles Prepared by Microemulsion Copolymerization

	starting microemulsion			nanoparticles			
					ligand content[c,d]		
	monomers	% **1** mol	init[a]	*D*,[b] nm	mol %	mmol/g tot[c]	mmol/g surf[d]
A	**1** + **2** + **3**	10	D	13	9	0.65	0.48
B	**1** + **2** + **3**	5	D	12	5	0.35	0.25
C	**1** + **2** + **3**[e]	11	D	20	11	0.73	0.31
D	**1** + **2**	10	D	15	10	0.71	0.35
E	**1** + **2**	15	D	15	10	0.61	0.35
F	**1** + **2** + **3**	11	P	22	7	0.53	0.23

[a] Initiator: P = $(NH_4)_2S_2O_8$/TMDAM; D = DMPA. [b] Average diameter determined by QELS and TEM (±10%). [c] Determined by elemental analysis. [d] Amount of cyclam surface residues deduced from spectrophotometric titration. [e] Polymerization performed in the presence of 2 equiv of NaOH per **1**.

photoinitiator (DMPA: 2,2-dimethoxy-2-phenylacetophenone) or a water-soluble redox system (ammonium persulfate/tetramethyldiaminomethane).[12−14] In every case, polymerization readily takes place, reaching 100% conversion of all monomers within a few hours, and leads to stable translucent aqueous suspensions of nanoparticles: the average diameters, determined by quasi-elastic light scattering and electron microscopy, range from 12 to 22 nm (Table 1). The content of cyclam incorporated in the particles is deduced from elemental analysis and can be easily modulated from the amount of polymerizable macrocycle **1** initially introduced.

b. Characterization. Whatever the composition of the starting mixture of monomers (molar ratio, presence or absence of a cross-linking agent), DMPA-initiated copolymerizations in cationic surfactant-based microemulsions afford stable translucent aqueous suspensions of very small nanoparticles in the 12−15 nm diameter range, among the smallest ever described (Table 1; samples A, B, D, E). As illustrated by freeze-fracture electron microscopy in Figure 1a, these ultrafine particles are remarkly monodispersed with a very narrow size distribution. Slightly larger particles, with a mean diameter of 20 nm, are obtained in basic medium, i.e., when the macrocycle is not protonated (sample C). A pH-dependent location of the polymerizable ligand **1** in between the oil droplet core and the interfacial layer may account for these variations of size. In basic medium, the neutral aza macrocycle is preferentially solubilized within the oil droplet core and does not significantly take part in the interfacial stabilization: in this case, the particle size is quite similar to those obtained by polymerization of styrene alone under the same experimental conditions. On the other hand, in a neutral medium, the aza macrocyclic comonomer **1** is protonated and get enriched at the oil−water interface: it contributes to the droplet surface coverage, thus giving rise to a decrease of the particle size according to the previously proposed geometrical Antonietti−Wu model.[10,33]

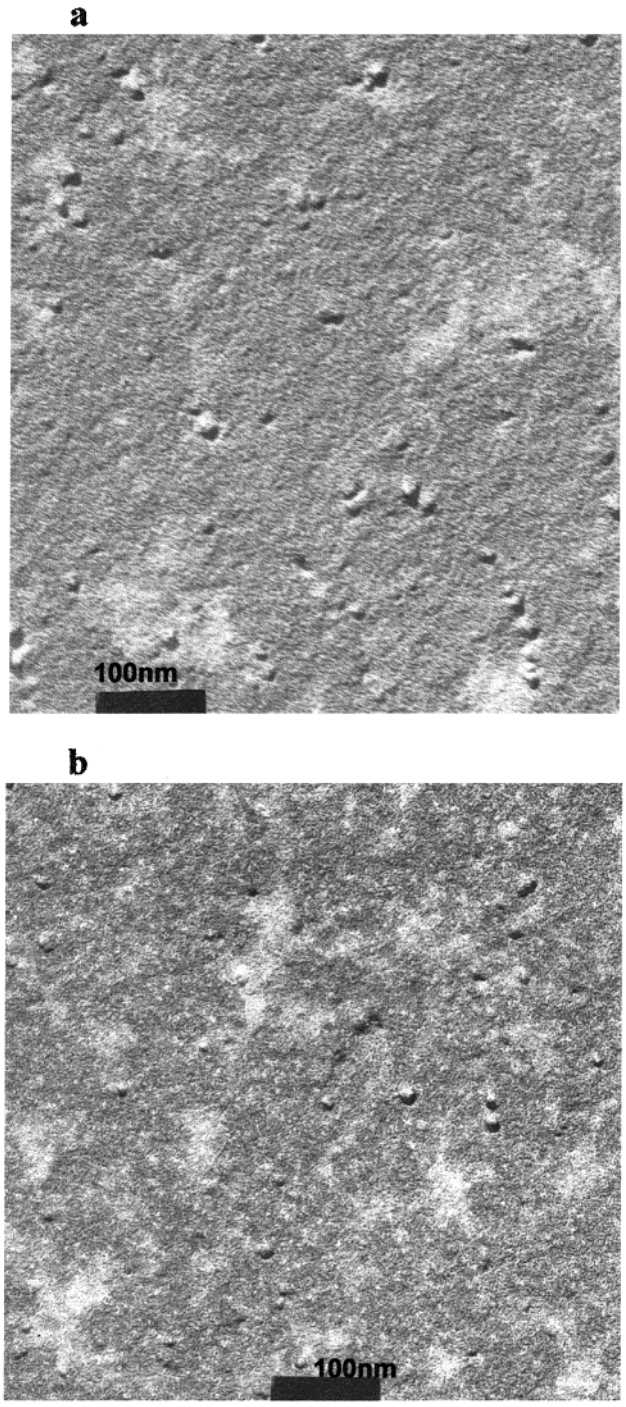

Figure 1. Freeze-fracture electron microscopy (×102 000): (a) suspension of cyclam-functionalized nanoparticles A (DTAB 0.15 wt %); (b) surfactant-free suspension of Cu−cyclam-functionalized nanoparticles A−Cu(II) (0.6 mmol of Cu/g of polymer).

The molar ratio of polymerizable cyclam derivative **1** incorporated in the nanoparticles reaches up to 11%,

i.e., 0.7−0.75 mmol of cyclam residues per gram of polymer (Table 1). When higher concentrations are introduced in the starting microemulsions, **1** is only partly incorporated within the particles (sample E: 15% introduced, 10% incorporated). In the latter case, polymerization of **1** partly takes place in water, giving rise to water-soluble low-molecular-weight polymers which are removed during the purification.

Remarkably, the amount of cyclam ligand that can be incorporated without increasing the particle size is comparatively much higher than in previously reported bipyridine-functionalized nanoparticles (only 2.5−3.5 mol %, i.e., 0.23−0.3 mmol of ligand/g for 25−35 nm particles).[16]

c. Colloidal Stability. The aqueous suspensions of cyclam-functionalized nanoparticles prepared in the cationic surfactant DTAB-based microemulsions using the nonionic photoinitiator DMPA are remarkably stable: the as-prepared suspensions can be stored for more than 6 months without particle aggregation. Furthermore, these colloidal suspensions tolerate changes of pH, from pH 2 to 8, as well as changes of ionic strength. They are stable in the presence of added electrolytes, giving no flocculation up to 5 mol/L chloride or nitrate salts of monovalent or divalent cations (sodium, calcium, copper, zinc, etc.) and up to 0.5 mol/L of sodium sulfate. Interestingly, these colloidal suspensions remain stable without particle aggregation when the surfactant concentration is reduced to 0.15 wt % by dialysis, as illustrated by the TEM picture in Figure 1.

It is worth noticing that, considering the copolymerization of the aza macrocyclic monomer **1**, cationic surfactant-based microemulsions should be used since copolymerization in "classical SDS microemulsions" prepared with the well-known sodium dodecyl sulfate anionic surfactant[12,13,34] was found to give unstable suspensions of larger particles. The formation of ion pairs between the macrocycle **1**, protonated at neutral pH, and the anionic surfactant may account for these results. In the same way, similar ionic interactions may explained that nanoparticles resulting from persulfate-initiated polymerization (sample F) slowly aggregate and finally give rise to large particles with a broad size distribution after a few weeks. Consequently, nonionic radical initiators, like DMPA used in the present work, should be preferred for the synthesis of cyclam-functionalized nanoparticles.

II. Copper Binding Capacity of Cyclam-Functionalized Nanoparticles. a. Binding Capacity and Characterization of the Cu(II)−Cyclam Nanoparticles. Owing to the high affinity of cyclam for cupric ions,[22,23,32] copper elemental analysis has been used to estimate the metal binding capacity of the cyclam-functionalized nanoparticles. Complexation experiments, performed at room temperature in the presence of stoichiometric amounts of copper nitrate, clearly illustrate the high binding capacity and ligand accessibility (Table 2). Whatever the starting suspension, the complexation of more than 85% of the cyclam residues is reached with copper contents of up to 0.6−0.65 mmol/g in the isolated particles. For 12−15 nm particles, complete complexation is achieved under stoichiometric conditions (complexation yield >95%).

Remarkably, the particle size remains unchanged after complexation (Table 2). The freeze-fracture electron microscopy picture given in Figure 1b shows individual particles, with a very narrow size distribution, well dispersed all over the sample and the absence of aggregates.

Table 2. Ligand Accessibility and Metal Binding Capacity Deduced from Cu(II) Binding Experiments and Spectroscopic Studies

nanolatex	A	B	C	D
cyclam content (mmol/g)[a]	0.65	0.35	0.73	0.71
accessible cyclam (mmol/g)[b]	0.48	0.25	0.31	0.35
% cyclam on the surface	74	72	42	50
Cu−cyclam max (mmol/g)[c]	0.62	0.32	0.61	0.58
diameter (nm)[d]				
starting particles	13	12	20	15
+ Cu(II)	13	12	22	17
n cyclam/particle[e]	450	190	1840	760
n cyclam surf/particle[e]	335	140	780	375
n Cu−cyclam max/particle[e]	430	175	1540	615
specific area (m^2/g)	460	500	300	400
cyclam surf (m^2/g)[f]	230	125	150	170

[a] From elemental analysis. [b] Outer cyclam residues deduced from spectroscopic titration in dilute medium. [c] Under stoichiometric conditions, deduced from Cu−cyclam complexe absorption and Cu elemental analysis. [d] Mean diameter of the particles before and after copper complexation, determined by QELS and TEM ± 10%. [e] Number of cyclam and Cu−cyclam moieties per particle calculated assuming a density of 1. [f] Specific area of surface−cyclam residues assuming an area of 0.8 nm^2 per cyclam residue.

Particles as small as 12−13 nm and containing up to 400−450 Cu(II) per particle are thus readily obtained (Table 2). The cation binding capacity of these cyclam-functionalized nanoparticles, prepared by a straightforward one-step polymerization procedure, can be compared to those of the more sophisticated dendrimers: for example, generation six[28] and generation eight[27] poly(amidoamine) dendrimers, PAMAM, bind respectively 64 and 153 Cu(II) ions per molecule, i.e., 1.1 and 0.65 mmol/g. It is worth noticing that the copper concentration in our 12−13 nm particles, i.e., 350−450 mmol per nm^3, is very close to those obtained in the dendritic structures (320−420 mmol per nm^3, calculated from the respective dendrimers diameters: 6.7 and 9.7 nm).[27,28]

b. Stability of the Cu(II)−Cyclam Nanoparticles. The deep violet translucent suspensions of Cu−cyclam functionalized nanoparticles exhibit a remarkable colloidal stability: they can be stored for months and do not aggregate in the presence of up to 2 mol/L chloride or nitrate salts. Moreover, neither flocculation nor copper decomplexation is observed when the pH is lowered down to pH 3. Furthermore, the surfactant can be entirely removed by dialysis without destabilization affording surfactant-free suspensions of nanoparticles (TEM picture, Figure 1b). Electrostatic stabilization arising from ionic repulsions between the positively charged nanoparticles may account for the colloidal stability of the aqueous suspensions of Cu−cyclam nanoparticles.

III. Ligand Accessibility. a. Spectrophotometric Studies of the Complexation: Discrimination between Outer and Inner Ligands. Taking advantage of the transparency of the suspensions, the amount of Cu(II)−cyclam complex in the nanoparticles is easily determined spectrophotometrically from its characteristic absorbance: quantitative and reproducible measurements, in good agreement with copper elemental analyses, are obtained by using an integrating sphere to collect and integrate the scattered light. These spectroscopic studies give useful information on the ligand accessibility. Thus, upon progressive addition of a dilute 0.01 M solution of Cu(II), the suspensions of

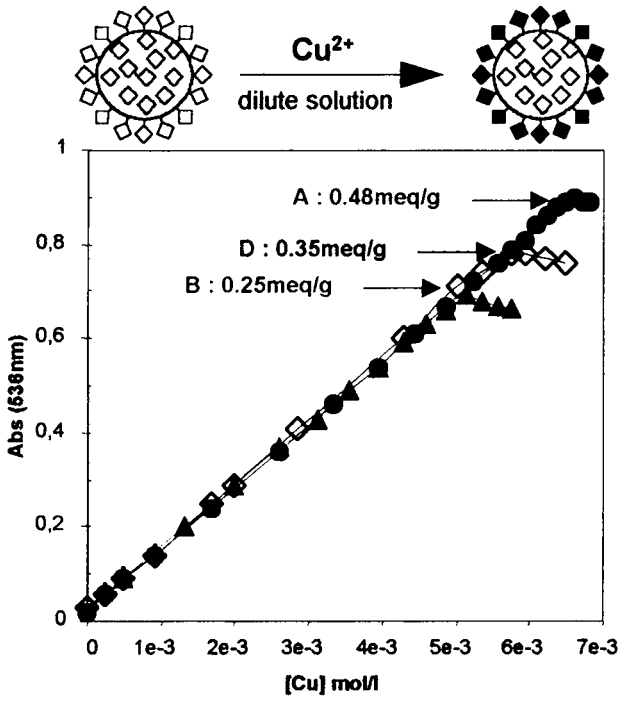

Figure 2. Spectrophotometric titration of cyclam upon progressive addition of dilute $Cu(NO_3)_2$ (0.01 M) to suspensions A, B, and D. Instantaneous absorbance of Cu−cyclam complex at 536 nm vs copper concentration.

cyclam-functionalized particles instantaneously turn violet, indicating that complexation readily takes place even at very low copper concentrations. The suspensions exhibit a maximum absorption wavelength at 536 nm (ϵ = 134 L mol^{-1} cm^{-1}) very close to those of the monomeric Cu(II)/**1** complex (537 nm, 134 L mol^{-1} cm^{-1}), indicating that the binding to the nanoparticles does not modify the structure of the complex. As can be seen in Figure 2, the absorbance of the copper complex linearly increases up to a maximum value that corresponds to the instantaneous complexation of all the accessible cyclam moieties in dilute medium. The amount of cyclam residues on the surface can thus be readily deduced from spectrophotometric titration and compared for various suspensions (Table 2, Figure 2).

Furthermore, in the case of nanoparticles containing the lowest amounts of accessible cyclam moieties, the spectrophotometric studies clearly indicate that two complexation processes take place: a rapid "solution-like" complexation process involving the outer cyclam residues located near the surface, which occurs at the minute time scale in dilute medium, and a slow diffusion-limited complexation process involving the inner cyclam residues entrapped within the core of the particles. Thus, as illustrated in Figure 3a, in the case of 20 nm particles, about 42% of the cyclam moieties are accessible for complexation at the minute time scale in dilute medium (first plateau). A second complexation step then proceeds much slowly and complete Cu(II) binding is achieved after several hours. Upon further stepwise additions of dilute copper, the same scenario is observed: no instantaneous complexation (second and third plateau) and then progressive complexation for longer reaction times; the higher the concentration of Cu−cyclam in the particles, the longer the complexation time. Moreover, in agreement with a diffusion-limited complexation process for the inner cyclam moieties, the higher the copper concentration in solution, the higher

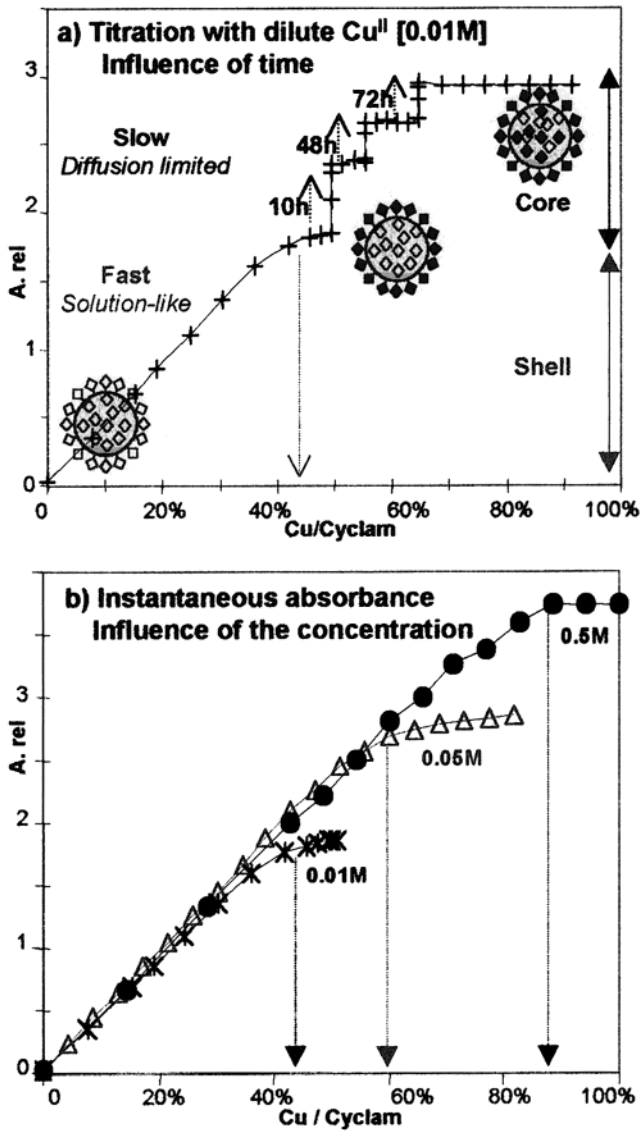

Figure 3. Spectrophotometric titration of cyclam upon progressive addition of $Cu(NO_3)_2$ to suspension C (nanoparticles average diameter: 20 nm). Relative absorbance (per gram of suspension) vs equivalents of Cu added per cyclam. (a) Variation of absorbance with time upon addition of dilute 0.01 M $Cu(NO_3)_2$. (b) Instantaneous absorbance upon addition of $Cu(NO_3)_2$ at various concentrations.

the extent of instantaneous complexation at a given Cu(II) per cyclam ratio (Figure 3b). It is worth noticing that the maximum complexation yield, 85%, is reached at the minute time scale upon addition of stoichiometric amounts of Cu(II) as a 0.5 M solution, i.e., about 2.5 × 10^{-2} mol of Cu(II)/L in the suspensions.

Similar behaviors have been observed for ultrafine 12−15 nm nanoparticles containing high densities of outer cyclam residues (e.g., suspensions A and B) with a much minor contribution of the diffusion-limited process: the overall maximum complexation yield in dilute medium is about 85−90% including 70−75% of outer cyclam residues involved in a rapid Cu(II) binding process and only 10−15% of inner cyclam residues involved in a diffusion-limited complexation process. A complexation yield of up to 95% is achieved at the minute time scale upon addition of stoichiometric amounts of Cu(II) as a 0.5 M solution.

These results clearly shed light on the huge improvement of the ligand accessibility brought by decreasing

the particle size with a clear correlation between the percentage of accessible ligands and the surface-to-volume ratio.

It is worth noticing that, in a previously reported study of bipyridine-functionalized nanoparticles,[16] the authors observed "a slow approach to the finite color in the presence of divalent metallic cations": considering the size of their particles (25−35 nm), the diffusion-limited process evidenced above, involving inner bipyridine moieties entrapped within the microgel particles core, may well account for these observations.

b. Relationship between the Ligand Accessibility and the Polymerization Conditions. The results summarized in Tables 1 and 2 clearly demonstrate that the density of ligand on the particle surface depends on the copolymerization conditions and can be readily modulated. The cyclam accessibility is remarkably enhanced when the particle size decreases: thus, for similar compositions of the starting microemulsions, the percentage of cyclam residues located on the surface is much higher on 12−15 nm particles resulting from an "oil-initiated" polymerization at neutral pH (sample A, 75% of the whole cyclam residues) than on 20 nm particles resulting from a "water-initiated" polymerization at neutral pH or an "oil-initiated" polymerization at basic pH (samples C and F, only 40−45%). Furthermore, as expected, for comparable sizes (13−15 nm) and comparable cyclam contents, the amount of accessible ligands is significantly increased by cross-linking (suspensions D and A: 0.35 and 0.48 mmol/g prepared respectively in the absence and in the presence of 40% of cross-linking agent **3**). Whatever the overall content of cyclam, highly cross-linked microgel-type nanoparticles exhibit a remarkable ligand accessibility since the complexation of about 75% of the whole cyclam residues is achieved in dilute medium at the minute time scale (Table 2, suspensions A and B).

In agreement with previously reported studies, these observations can be explained by considering that the mechanism of copolymerization in microemulsion depends on the microenvironment and especially on the relative local concentrations of the monomers at the region where the initiation step takes place.[9,10−13,17] When the comonomer is preferentially located at the oil−water interface, like **1** in neutral medium, and when the free radicals are produced within the oil droplets core (oil-soluble initiator DMPA), the polymerization proceeds first with styrene until the comonomer concentration at the reaction loci becomes sufficient and finally leads to a high density of hydrophilic ligand residues in the particle shell.[12] The effect of the preferential orientation is much pronounced in the presence of a lipophilic cross-linking agent since kinetic prevails over thermodynamic.[10] In basic medium, the nonprotonated comonomer **1** is preferentially located within the oil droplets core: the copolymerization takes place randomly and leads to a random distribution of the cyclam residues over the whole particle volume, thus resulting in a restricted ligand accessibility.[12]

IV. Selectivity of Cyclam-Functionalized Nanoparticles. a. Competition Experiments. The selectivity of the cyclam-functionalized nanoparticles for Cu(II) and their binding capacity for other divalent cations were studied by performing competition experiments with various metallic cations (M: Ni(II), Co(II), Zn(II)). In every case, elemental analyses of the metals content in the isolated particles show that complete complexation of Cu(II) does take place even in the presence of a very large excess of competing ion (M/Cu = 1000; M/cyclam = 100; Table 3). These results demonstrate the remarkable selectivity of the cyclam-functionalized nanoparticles for cupric ions: the ligand selectivity is retained on particles. The nanoparticles also bind Ni(II), Co(II), and Zn(II) with complexation yields, reaching about 55% of the remaining free-cyclam moieties. Moreover, the surfactant and the excess of unreacted competing ions are easily removed by dialysis without destabilization or decomplexation. Competition experiments thus give access to stable surfactant-free colloidal suspensions of "bimetallic" nanoparticles in which the molar ratio of the two metallic cations can readily be modulated.

Table 3. Selectivity for Cupric Ions from Competition Experiments[a,b]

competing cation (M)	Ni(II)	Zn(II)	Co(II)
M (mmol/g)	0.39	0.37	0.39
Cu (mmol/g)	0.08	0.05	0.05
Cu complexation yield (%)	>98	>98	>98
M/cyclam (%)	55	52	55
M + Cu/cyclam (%)	65	60	60
n M(II) per particle[c]	985	935	985
n Cu(II) per particle[c]	200	125	125

[a] Starting suspension C: 20 nm. [b] Experimental conditions: Cu/cyclam = 0.1−0.15, M/cyclam = 100, M/Cu = 1000. [c] Number of Cu or M residues per particle calculated assuming a density of 1.

b. Preparation of Core−Shell Type Bimetallic Nanoparticles by Cation Exchange. Bimetallic nanoparticles with adjustable ratios of two cations, M^{2+} and Cu^{2+}, can alternatively be prepared by exchanging a given cation M^{2+} (Zn^{2+}, Co^{2+}, Ni^{2+}) for cupric ion. The cation exchange is readily monitored by spectrophotometric titration of the copper−cyclam complex. As illustrated in Figure 4, in the case of 20 nm particles, the displacement of Zn(II) by Cu(II) readily takes place upon addition of dilute copper nitrate to a colorless aqueous suspension of Zn−cyclam nanoparticles. In dilute medium, copper complexation is quantitative within a few hours (2−5 h) up to the substitution of 65% of Zn and then reaches a plateau with longer equilibrium times. Nanoparticles containing adjustable Cu/Zn ratios, from 0 to 2, are thus readily accessible by addition of controlled Cu aliquots. Remarkably, in dilute medium, the maximum substitution yield corresponds to the complexation of about 45% of the whole cyclam moieties by Cu(II): this value corresponds to the amount of accessible ligands located on the surface for the 20 nm particles studied (Table 2, suspension C). These results clearly indicate that, in dilute medium, the substitution is limited to the outer cyclam residues and therefore results in the production of core−shell type nanoparticles with a Cu-rich shell and a Zn-rich core.

Conclusion

Microemulsion copolymerization is a useful technique to produce ultrafine ligand-functionalized nanoparticles with high density of ligands and up to ca. 300 m^2 cyclam-functionalized surface per gram of polymer. One of the most outstanding features of copolymerization using microemulsion as reaction medium is the control of the surface characteristics. The spectroscopic study of the complexation process clearly indicates that the ligand accessibility is closely correlated with the particle size. Moreover, the properties of a selective ligand like

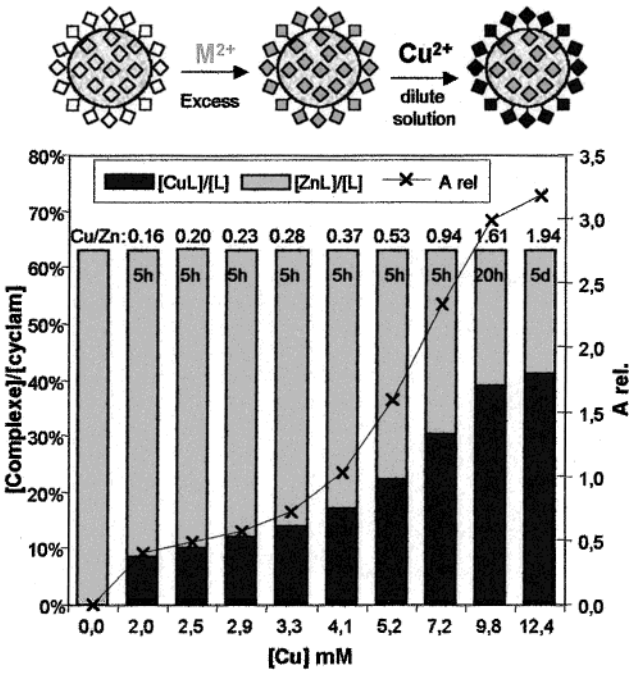

Figure 4. Replacement of Zn(II) by Cu(II) upon addition of a dilute solution of $Cu(NO_3)_2$ (0.01 M) to Zn(II)-loaded nanoparticles. Relative absorbance (per gram of suspension) at 536 nm at the equilibrium, molar ratios Cu−cyclam complex/cyclam and Zn−cyclam complex/cyclam vs copper concentration. Starting suspension C−Zn(II) [20 nm, 0.37 mmol Zn/g, molar ratio Zn/cyclam = 0.62] obtained by reaction of an excess of zinc nitrate with suspension C.

cyclam are not influenced by the binding to the particles so that a real "solution-like" chemistry, very close to classical supramolecular chemistry, becomes accessible on colloidal polymer nanoparticles. A comparably simple technique of microemulsion polymerization results in polymer nanomaterials with properties very similar to the more sophisticated dendrimers.[27,28] Considering their very large specific area up to ca. 450 m^2/g, the ligand accessibility and selectivity, metal-complexing nanoparticles are very attractive supports for a variety of applications like specific recovery, sensors, and the development of new immobilized catalysts including atom transfer polymerization catalysts.[35] Moreover, as illustrated in this paper, such selective ligand-functionalized nanoparticles may also find promising applications in materials science for the development of new polymer composites.

References and Notes

(1) Sherrington, D. C. *J. Polym. Sci., Part A: Polym. Chem.* **2001**, *39*, 2364−2377.
(2) Bergbreiter, D. E. *J. Polym. Sci., Part A: Polym. Chem.* **2001**, *39*, 2351−2363.
(3) Ford, W. T. *React. Funct. Polym.* **1997**, *33*, 147−158.
(4) (a) Kirschning, A.; Monenschein, H.; Wittenberg, R. *Angew. Chem., Int. Ed.* **2001**, *40*, 650−679. (b) Blackburn, C. *Biopolymers (Peptide Science)* **1998**, *47*, 311−353. (c) Eames, J.; Watkinson, M. *Eur. J. Org. Chem.* **2001**, 1213−1224. (d) Ley, S. V.; Massi, A.; Rodriguez, F.; Horwell, D. C.; Lewthwaite, R. A.; Pritchard, M. C.; Reid, A. M. *Angew. Chem., Int. Ed.* **2001**, *40*, 1053−1055.
(5) Haag, R. *Chem. Eur.* **2001**, *7*, 327−335.
(6) Li, W.; Yan, B. *J. Org. Chem.* **1998**, *63*, 4092−4097.
(7) Hodges, I. C.; Hearn, J. *Langmuir* **2001**, *17*, 3419−3422.
(8) Guyot, A.; Hodge, P.; Sherrington, D. C.; Widdecke, H. *React. Polym.* **1991/1992**, *16*, 233−259.
(9) (a) Candau, F. In *Handbook of Microemulsion Science and Technology;* Kumar, P., Mittal, K. L., Eds.; Marcel Dekker: New York, 1999; Chapter 22, pp 679−712. (b) Candau, F. In *Polymerization in Organized Media*; Paleos, C. M., Ed.; Gordon and Breach Publishers: Philadelphia, 1992; Chapter 4, pp 215−282.
(10) Antonietti, M.; Basten, B.; Lohmann, S. *Macromol. Chem. Phys.* **1995**, *196*, 441−466.
(11) Capek, I. *Adv. Colloid Interface Sci.* **1999**, *80*, 85−149.
(12) Larpent, C.; Bernard, E.; Richard, J.; Vaslin, S. *Macromolecules* **1997**, *30*, 354−362.
(13) Larpent, C.; Bernard, E.; Richard, J.; Vaslin, S. *React. Funct. Polym.* **1997**, *33*, 49−59.
(14) Larpent, C.; Amigoni-Gerbier, S. *Macromolecules* **1999**, *33*, 9071−9073.
(15) Antonietti, M.; Lohmann, S.; Van Niel, C. *Macromolecules* **1992**, *25*, 1139−43.
(16) Antonietti, M.; Lohmann, S.; Eisenbach, C. D.; Schubert, U. S. *Macromol. Rapid Commun.* **1995**, *16*, 283−289.
(17) (a) Dreja, M.; Pyckhout-Hintzen, W.; Tieke, B. *Macromolecules* **1998**, *31*, 272−280. (b) Pyrasch, M.; Tieke, B. *Colloid Polym. Sci.* **2000**, *278*, 375−379.
(18) Favero, C.; Graillat, C.; Guyot, A. *Macromol. Symp.* **2000**, *150*, 235−240.
(19) Beauvais, R. A.; Alexandratos, S. D. *React. Funct. Polym.* **1998**, *36*, 113−123.
(20) Alexandratos, S. D.; Crick, D. W. *Ind. Eng. Chem. Res.* **1996**, *35*, 635−644.
(21) Bergbreiter, D. E.; Koshti, N.; Franchina, J. G.; Frels, J. D. *Angew. Chem., Int. Ed.* **2000**, *39*, 1039−1042.
(22) Altava, B.; Burgette, M. I.; Frias, J. C.; Garcia-Espana, E.; Luis, S. V.; Miravet, J. F. *Ind. Eng. Chem. Res.* **2000**, *39*, 3589−3595.
(23) Puanik, D. B.; David, V. A.; Morris, R. E.; Chang, E. L. *Energy Fuels* **1997**, *11*, 1311−1312.
(24) Blain, S.; Appriou, P.; Chaumeil, H.; Handel, H. *Anal. Chim. Acta* **1990**, *232*, 331−336.
(25) Blacker, N. C.; Findlay, P. H.; Sherrington, D. C. *Polym. Adv. Technol.* **2001**, *12*, 183−196.
(26) Angelino, M. D.; Laibinis, P. E. *J. Polym. Sci., Part A: Polym. Chem.* **1999**, *37*, 3888−3898.
(27) Diallo, M. S.; Balogh, L.; Shafagati, A.; Johnson, J. H., Jr.; Goddard, W. A., III; Tomalia, D. A. *Environ. Sci. Technol.* **1999**, *33*, 820−824 and references therein.
(28) Crooks, R. M.; Zhao, M.; Sun, L.; Chechik, V.; Yeung, L. K. *Acc. Chem. Res.* **2001**, *34*, 181−190 and references therein.
(29) Vassilev, K.; Ford, W. T. *J. Polym. Sci., Part A: Polym. Chem.* **1999**, *37*, 2727−2736.
(30) Cameron, J. H.; Graham, S.; Harvey, B. H.; Liggat, J. J.; McKee, A.; Soutar, I.; Scott, E. L. *React. Funct. Polym.* **1998**, *36*, 173−183.
(31) Wang, B.; Wasielewski, M. R. *J. Am. Chem. Soc.* **1997**, *119*, 12−21.
(32) Thöm, V. J.; Hosken, G. D.; Hancock, R. D. *Inorg. Chem.* **1985**, *24*, 3378−3381. (b) Alexander, V. *Chem. Rev.* **1995**, *95*, 273−275. (c) Christensen, J. J.; Eatough, D. J.; Izatt, R. M. *Chem. Rev.* **1974**, *74*, 351−384.
(33) Antonietti, M.; Bremser, W.; Müschenborn, D.; Rosenauer, C.; Schupp, B.; Schmidt, M. *Macromolecules* **1991**, *24*, 6636−6643.
(34) Guo, J. S.; Sudol, E. D.; Vanderhoff, J. W.; El-Aasser, M. S. *J. Polym. Sci., Part A: Polym. Chem.* **1992**, *30*, 691−702, 703−712.
(35) Hong, S. C.; Paik, H. J.; Matyjaszewski, K. *Macromolecules* **2001**, *34*, 5099−5102.

MA0113632